Altered heart rate variability in angiotensin II–mediated hypertension is associated with impaired autonomic nervous system signaling and intrinsic sinoatrial node dysfunction

Tristan W. Dorey, BSc, Motahareh Moghtadaei, PhD, Robert A. Rose, PhD

From the Department of Cardiac Sciences, Libin Cardiovascular Institute of Alberta, Cumming School of Medicine, University of Calgary, Calgary, Alberta, Canada, and the Department of Physiology and Pharmacology, Libin Cardiovascular Institute of Alberta, Cumming School of Medicine, University of Calgary, Calgary, Alberta, Canada.

BACKGROUND Hypertensive heart disease is associated with sinoatrial node (SAN) dysfunction and reductions in heart rate variability (HRV). Alterations in HRV could occur in association with changes in autonomic nervous system (ANS) activity, changes in SAN function and responsiveness to ANS agonists, or both. These relationships are unclear.

OBJECTIVE The purpose of this study was to investigate the roles of ANS signaling, intrinsic SAN function, and changes in HRV in a mouse model of angiotensin II (AngII)–mediated hypertensive heart disease.

METHODS Mice were treated with saline or AngII (2.5 mg/(kg·d)) for 3 weeks. ANS activity was assessed through HRV analysis of electrocardiograms collected in vivo by telemetry as well as direct recordings of vagal nerve activity and renal sympathetic nerve activity from anesthetized mice. The effects of the ANS agonists isoproterenol and carbachol on SAN function and beating interval variability were assessed from electrogram recordings in intact isolated atrial preparations and from spontaneous action potential recordings in isolated SAN myocytes.

RESULTS Time and frequency domain analysis demonstrates that mice infused with AngII had reduced HRV. AngII-infused mice had elevated renal sympathetic nerve activity while resting vagal nerve activity was unchanged. AngII caused an increase in SAN beating interval variability in isolated atrial preparations and isolated SAN myocytes. Furthermore, isolated atrial preparations and SAN myocytes from AngII-infused mice had impaired responses to both isoproterenol and carbachol.

CONCLUSION Reduced HRV in hypertension occurs in association with altered sympathovagal balance as well as intrinsic SAN dysfunction and reduced responsiveness of SAN myocytes to ANS agonists.

KEYWORDS Angiotensin II; Autonomic nervous system; Heart rate variability; Hypertension; Sinoatrial node

(Heart Rhythm 2020;17:1360–1370)

Introduction

Heart rate (HR) is determined by the intrinsic properties of the sinoatrial node (SAN) and is modulated by the autonomic nervous system (ANS).[1] The rate of spontaneous action potential (AP) generation within the SAN determines the intrinsic HR, which is then modified by the ANS. Specifically, the sympathetic nervous system (SNS) increases HR by increasing the rate of SAN AP firing after the activation of β-adrenergic receptors (β-ARs) on SAN myocytes by norepinephrine. Conversely, the parasympathetic nervous system (PNS) reduces HR via the release of acetylcholine, which activates muscarinic (M_2) receptors on SAN myocytes, leading to the slowing of spontaneous AP firing in the SAN.

It is well appreciated that beat-to-beat variation in HR (ie, variation in R-R interval on the electrocardiogram [ECG]), known as heart rate variability (HRV), is present in the healthy heart and that a robust level of HRV is a positive indicator of health status.[2,3] As such, reductions in HRV are associated with worsening prognosis in a number of conditions and disease states including hypertension.[4] HRV analysis has traditionally been used as a measure of changes in ANS activity in disease states such as hypertension. Specifically, HRV was thought to originate primarily from

This work was supported by the Canadian Institutes of Health Research (PJT 1666105 to Dr Rose). Mr Dorey holds a Canadian Institutes of Health Research Doctoral Research Award. **Address reprint requests and correspondence:** Dr Robert A. Rose, Libin Cardiovascular Institute of Alberta, Cumming School of Medicine, University of Calgary, GAC66, Health Research Innovation Centre, 3280 Hospital Dr NW, Calgary, Alberta, Canada T2N 4Z6. E-mail address: robert.rose@ucalgary.ca.

1547-5271/$-see front matter https://doi.org/10.1016/j.hrthm.2020.03.014

the ANS, with increases in PNS activity leading to increased HRV and increased SNS activity leading to reduced HRV.[2] More recently, however, it has become apparent that intrinsic SAN function can also affect beat-to-beat fluctuations in HR and that the intrinsic properties of SAN myocytes also determine HRV.[3,5]

SAN disease is prevalent in hypertension.[6,7] Consistent with this, we have recently shown that SAN disease in mice with angiotensin II (AngII)–induced hypertensive heart disease is associated with electrical remodeling (ie, impaired spontaneous AP firing in SAN myocytes) as well as structural remodeling (ie, fibrosis) of the SAN.[7] Hypertension has also been shown to be associated with alterations in ANS activity.[8,9] Collectively, these observations raise important questions about HRV in hypertension and the roles of the ANS and the SAN in producing beat-to-beat variations in HR in this disease setting.

Accordingly, the purpose of this study was to investigate the basis for changes in HRV in hypertension by assessing the roles of the ANS and intrinsic SAN function in changes in beating interval variability. Our studies were conducted in conscious mice, in intact (denervated) atrial preparations, and in isolated SAN myocytes. This multilevel approach to assessing HRV provides new insights into the basis for impaired HR regulation and reduced HRV in the setting of hypertensive heart disease.

Methods

An expanded methods section can be found in the Online Supplemental Materials.

Mice

This study used male wild-type C57Bl/6 mice between the ages of 10 and 15 weeks. Mice were treated with saline or AngII (2.5 mg/(kg•d)) for 3 weeks using osmotic minipumps (Alzet, Cupertino, California).[7] Blood pressure was measured by tail-cuff plethysmography.[7] Additional details are provided in the Online Supplement. All experimental procedures were approved by the University of Calgary Animal Care Committee and were in accordance with the guidelines of the Canadian Council on Animal Care.

Telemetry studies

Telemetric recordings were used to measure ECGs and activity levels in conscious, freely moving mice as we have described previously.[10] Additional details are provided in the Online Supplement.

Vagal parasympathetic and renal sympathetic nerve recordings

Renal sympathetic nerve activity recordings were measured by multifiber recording directly from the renal nerve. Vagal nerve activity recordings were obtained from the right cervical vagus nerve. All recordings were made using custom-made bipolar silver wire electrodes. Additional details are provided in the Online Supplement.

Plasma norepinephrine

Circulating norepinephrine levels were measured from plasma samples obtained from saline- and AngII-infused mice by using a commercially available enzyme immunoassay kit (Abnova, Taiwan).

Electrogram recordings in isolated atrial preparations

Intact, denervated atrial preparations containing the SAN were prepared as described previously.[7,11] Beating atrial preparations were superfused with Krebs solution at 37°C. ECGs were acquired using needle electrodes (Grass Technologies, Quincy, Massachusetts) placed in each atrial appendage. Further details are available in the Online Supplement.

AP recordings in isolated SAN myocytes

SAN myocytes were isolated as described previously.[7,12] Spontaneous APs were recorded using the perforated patch clamp technique in the current clamp mode. Further details are available in the Online Supplement.

HRV analysis

HRV was assessed using time and frequency domain analysis from telemetric ECG recordings in vivo, from electrogram recordings in atrial preparations, and from spontaneous APs in SAN myocytes. All data were analyzed using customized software written in MATLAB software (MathWorks, Natick, Massachusetts) as we have described previously.[10] Further details are available in the Online Supplement.

Statistical analysis

All data are presented as mean ± SEM. Data were analyzed using the Student *t* test, 2-way analysis of variance with a Holm-Sidak post hoc test, or 2-way repeated measures analysis of variance with a Holm-Sidak post hoc test as indicated in each figure legend. $P<.05$ was considered significant.

Results

Effects of AngII on HRV and SAN function in vivo

As expected, AngII infusion led to hypertension with increases in systolic blood pressure (Online Supplemental Figure 1). Telemetric HR data demonstrate reduced R-R interval (ie, increased HR) in AngII-infused mice (Figure 1A). This is evident by lower circadian variability over 48 hours (Figure 1B) and reduced average R-R intervals during day (7:00 AM to 7:00 PM) and night (7:00 PM to 7:00 AM) phases of the diurnal cycle (Figure 1C). There were no differences in activity levels between saline- and AngII-infused mice during day or night hours (Figure 1D). R-R interval histograms obtained over 48 hours illustrate that variability in R-R interval is reduced in AngII-infused mice (Figure 1E). Standard deviation of N-N intervals (SDNN) and the root mean squared of successive differences (RMSSD) were reduced during low and high activity in AngII-infused mice (Figures 1F and 1G). There were no

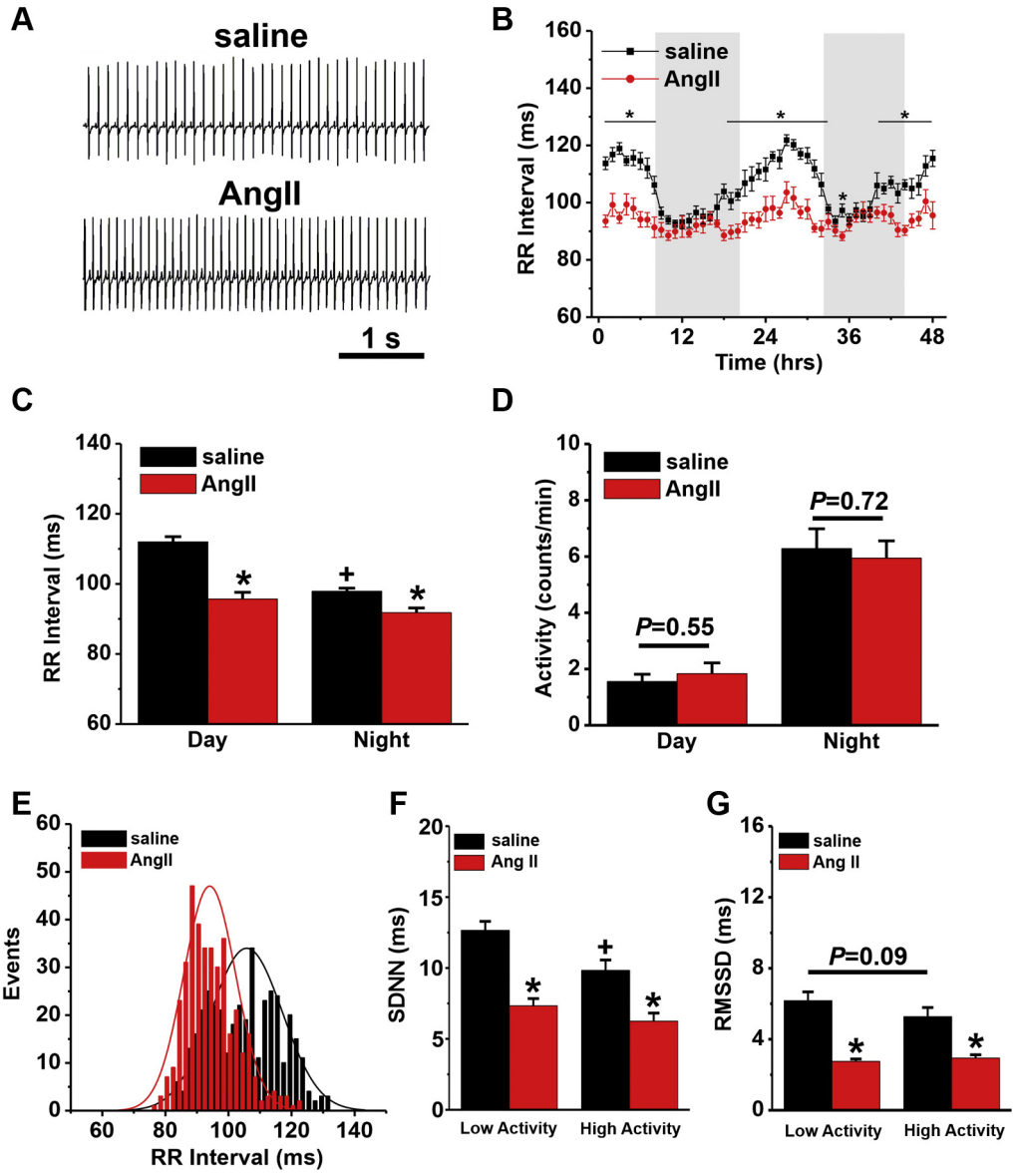

Figure 1 Time domain analysis of heart rate variability (HRV) in Angiotensin II (AngII)-infused mice. **A:** Telemetric ECG recordings from saline- and AngII-infused mice during the low activity phase. **B:** R-R fluctuations in mice infused with saline or AngII over a 48-hour period. Gray shading indicates nighttime hours. *$P<.05$ vs saline by 2-way analysis of variance (ANOVA) with the Holm-Sidak post hoc test. **C and D:** Summary of the mean R-R interval (panel C) and average activity levels (panel D) in saline- and AngII-infused mice during day and night cycles. **E:** Representative R-R histogram for saline- and AngII-infused mice during the low activity phase. **F and G:** Summary standard deviation of N-N intervals (SDNN) (panel F) and root mean squared of successive differences (RMSSD) (panel G) in saline- and AngII-infused mice in low and high activity phases. For panels C–G, *$P<.05$ vs saline within diurnal or activity phase; $^{+}P<.05$ vs day or low activity phase within treatment group by 2-way ANOVA with the Holm-Sidak post hoc test. n=8 saline-infused mice and n=8 AngII-infused mice.

differences between low activity and high activity phases in the presence of AngII for SDNN ($P=.11$) or RMSSD ($P=.42$).

Next, we examined the effects of AngII infusion on HRV and SAN arrhythmogenesis after ANS blockade (via intraperitoneal injection of atropine and propranolol) in vivo (Figure 2). R-R interval was prolonged in AngII-infused mice after ANS blockade (Figures 2A and 2B), indicating impaired intrinsic SAN function. Furthermore, AngII caused increases in SDNN and RMSSD in the presence of ANS blockade (Figure 2C), indicating increased intrinsic SAN variability. Consistent with these observations, the incidence of sinus pauses was increased in mice infused with AngII (Figure 2E).

Power spectral density plots (baseline conditions) demonstrate that total power was reduced in AngII-infused mice (Figure 3A). Atropine injection (PNS blockade) decreased R-R interval while propranolol injection (SNS blockade) increased R-R interval in saline- and AngII-infused mice (Figure 3B). The R-R interval was lower after propranolol injection in AngII-infused mice. Frequency domain analysis shows that AngII-infused mice had reduced

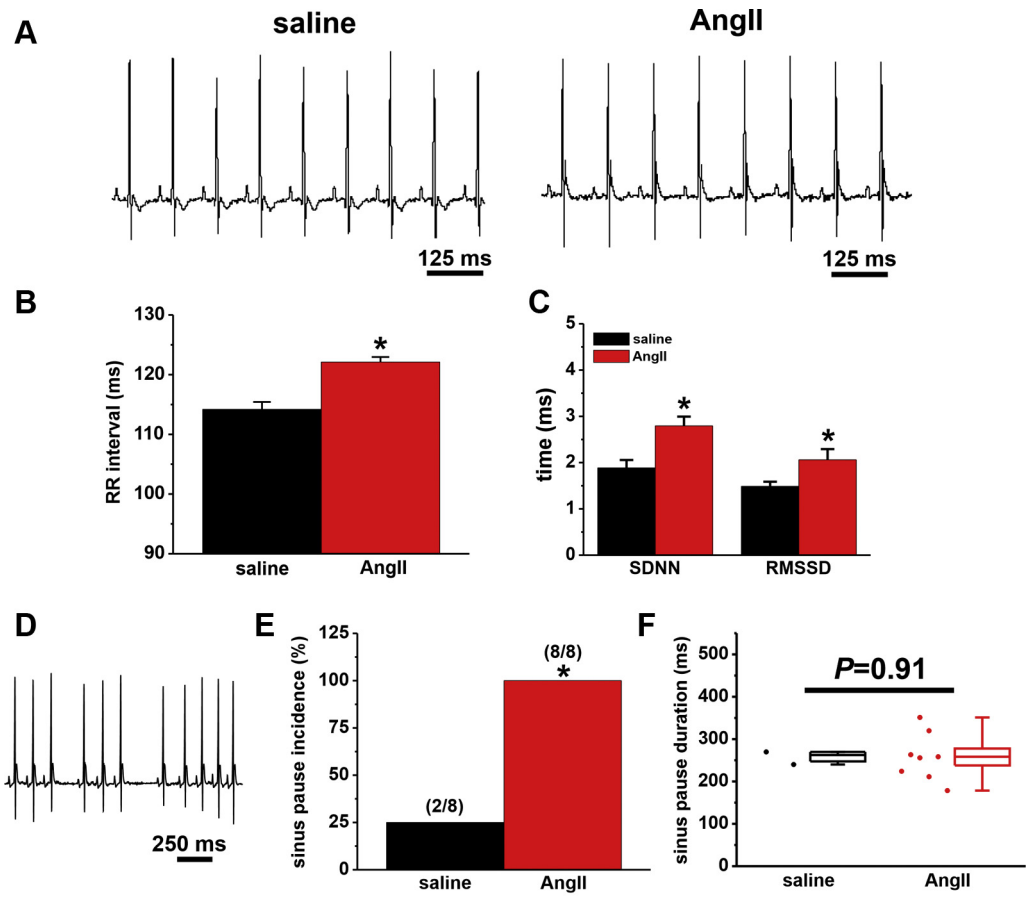

Figure 2 Effects of Angiotensin II (AngII) on heart rate, heart rate variability (HRV), and sinus pauses after autonomic nervous system (ANS) blockade in conscious mice. **A:** Telemetric ECG recordings from saline- and AngII-infused mice after intraperitoneal injection of propranolol (10 mg/kg) and atropine (10 mg/kg). **B:** Effects of AngII on R-R interval after ANS blockade. **C:** Effects of AngII on standard deviation of N-N invervals (SDNN) and root mean squared of successive differences (RMSSD) after ANS blockade. For panels B and C, *$P<.05$ vs saline by Student t test. n=8 saline-infused mice and n=8 AngII-infused mice. **D:** Telemetric ECG recording from an AngII-infused mouse illustrating the occurrence of sinus pauses. **E:** Incidence of sinus pauses in saline- and AngII-infused mice. Numbers in parentheses indicate the number of mice in each group that developed sinus pauses. *$P<.05$ vs saline by Fisher exact test. **F:** Sinus pause duration in the subset of saline (n=2)– and AngII (n=8)–infused mice that exhibited sinus pauses.

total power (Figure 3C), high frequency (HF) power (Figure 3D), and low frequency (LF) power (Figure 3E). Atropine decreased total, HF, and LF power in saline- and AngII-infused mice (Figures 3C–3E). Propranolol decreased total, HF, and LF power in saline-infused mice (Figures 3C–3E). In contrast, there was a trend ($P=.07$) toward reduction in total power (Figure 3C), no change ($P=.94$) in HF power (Figure 3D), and a reduction in LF power (Figure 3E) after propranolol injection in AngII-infused mice. These data indicate a reduction in PNS activity and a shift toward increased SNS activity in AngII-infused mice.

Effects of AngII on autonomic nerve activity

To directly assess the effects of AngII on sympathetic and parasympathetic nerve activity, we obtained vagal and renal sympathetic nerve recordings in anesthetized mice in vivo (Figure 4). Vagal nerve spike frequency (Figures 4A and 4B) and the respiratory component of vagal nerve activity (Figure 4C) were not different between saline- and AngII-infused mice. In contrast, renal sympathetic nerve burst frequency (Figures 4D and 4E) and integrated renal sympathetic nerve activity (Figure 4F) were each increased in AngII-infused mice. In agreement with increases in sympathetic nerve activity, plasma norepinephrine was increased in AngII-infused mice (Figure 4G).

Effects of ANS agonists on isolated atrial preparations in AngII-infused mice

In isolated atrial preparations lacking neural inputs, electrogram recordings (Figure 5A) and tachograms (Figure 5B) demonstrate that AngII-infused mice had increases in interbeat interval (IBI) (Figure 5C) and beating interval variability (SDNN) (Figure 5D) under baseline conditions. Isoproterenol (ISO) reduced SDNN in both groups; however, SDNN remained greater in atrial preparations from AngII-infused mice (Figure 5D). Carbachol

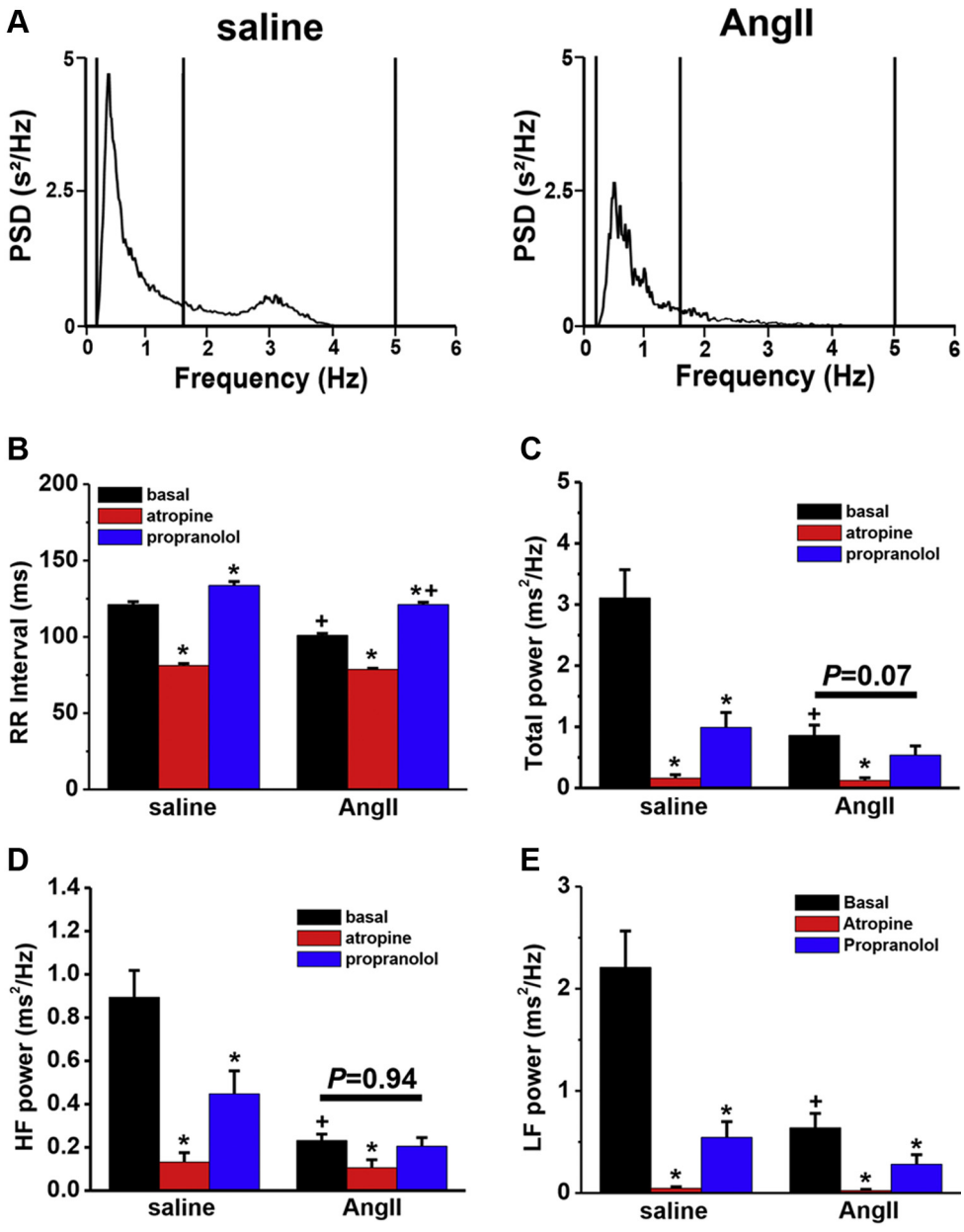

Figure 3 Effects of autonomic nervous system (ANS) blockers on R-R interval and frequency domain measures of heart rate variability (HRV) in Angiotensin II (AngII)-infused mice. **A:** Representative power spectral density plots for saline- and AngII-infused mice. **B–E:** Summary data illustrating the effects of atropine (10 mg/kg) or propranolol (10 mg/kg) on R-R interval (panel B), total power of the HRV spectra (panel C), high-frequency power (panel D), and low-frequency power (panel E) in saline- and AngII-infused mice. *$P<.05$ vs basal condition within treatment group; $^{+}P<.05$ vs saline within injection condition by 2-way repeated measures ANOVA with a Holm-Sidak post hoc test. n=8 saline-infused mice and n=8 AngII-infused mice.

(CCh) increased SDNN in both groups; however, the magnitude of the increase was smaller in atrial preparations from AngII-infused mice. Dose-response curves show that the half maximal effective concentration (EC_{50}) for the effects of ISO (7.9 ± 0.01 μM vs 8.31 ± 0.02 μM) and CCh (5.66 ± 0.1 nM vs 6.55 ± 0.1 nM) on beating rate were each increased ($P<.05$) in atrial preparations from AngII-infused mice (Figures 5E and 5F). These data demonstrate that SAN responsiveness to ANS agonists is impaired after AngII infusion.

Effects of ANS agonists on isolated SAN myocytes in AngII-treated mice

Finally, we investigated variability in intrinsic SAN myocyte electrophysiology and responsiveness to ANS agonists in AngII-infused mice. Spontaneous AP recordings in SAN myocytes isolated from AngII-infused mice showed increased baseline IBI and beating rate variability (Online Supplemental Figures 2A–2C). Furthermore, SDNN, the coefficient of variation (COV), and standard deviations (SD1 and SD2) from Poincaré plot analysis (Online

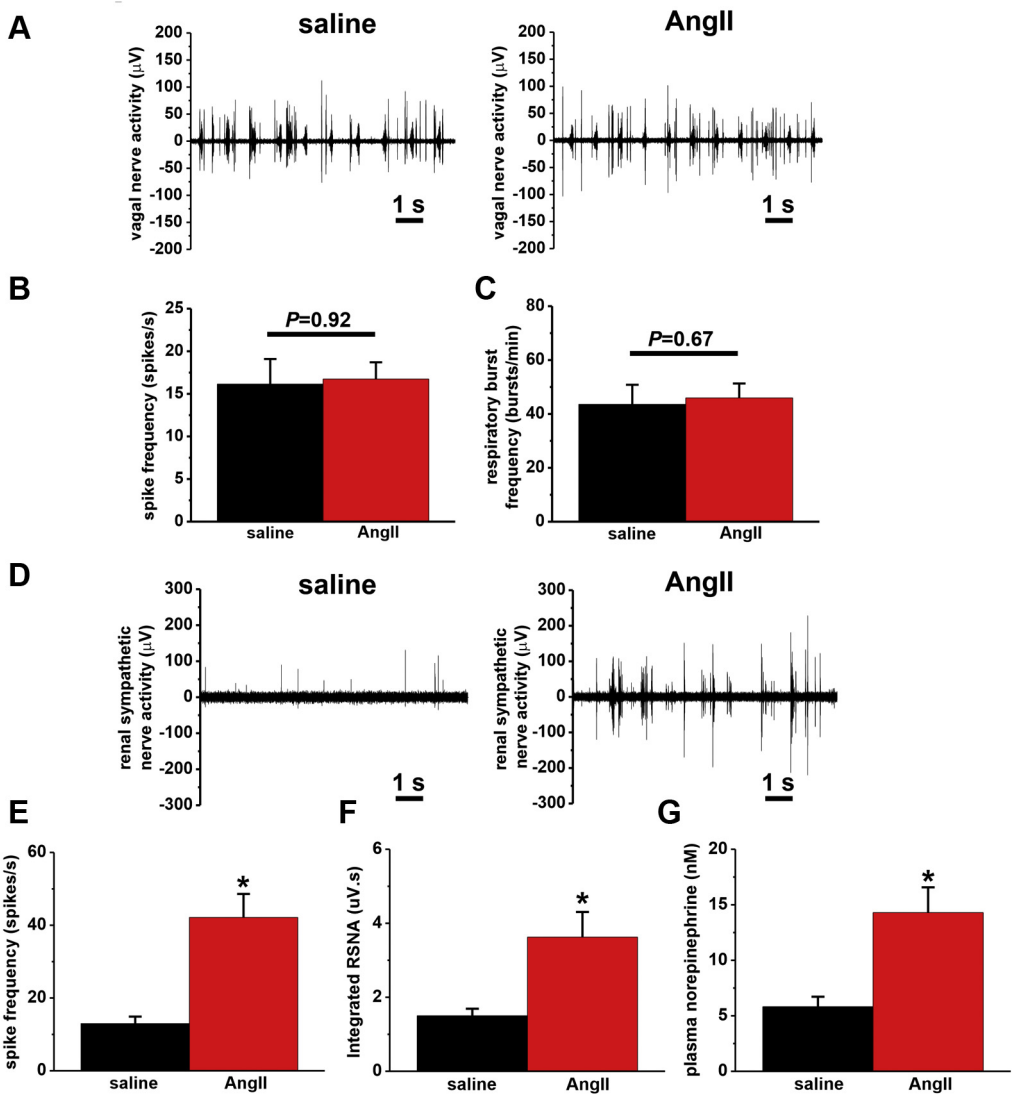

Figure 4 Assessment of vagal parasympathetic nerve and renal sympathetic nerve activity in anesthetized Angiotensin II (AngII)-infused mice. **A:** Representative vagal nerve activity (VNA) recordings from saline- and AngII-infused mice. **B and C:** Summary data illustrating no differences in VNA spike frequency (panel B) or respiratory burst frequency (panel C) between saline (n=8)– and AngII (n=8)–infused mice. **D:** Representative renal sympathetic nerve activity (RSNA) recordings from saline- and AngII-infused mice. **E and F:** Summary of the effects of AngII infusion on RSNA spike frequency (panel E) and integrated RSNA (panel F). *P<.05 vs saline by Student t test. n=8 saline-infused mice and n=8 AngII-infused mice. **G:** Plasma norepinephrine concentrations in saline- and AngII-infused mice. *P<.05 vs saline by Student t test. n=10 saline-infused mice and n=10 AngII-infused mice.

Supplemental Figures 2D–2F) were each increased in SAN myocytes from AngII-infused mice.

ISO decreased IBI in SAN myocytes (Figures 6A and 6B); however, the magnitude of this effect was smaller in AngII-infused mice (Figure 6C). ISO reduced SDNN (Figure 6D) and COV (Figure 6E) in isolated SAN myocytes from saline- and AngII-infused mice. Nevertheless, SDNN remained larger after the application of ISO in AngII-infused mice. COV after the addition of ISO was not different between groups. Poincaré plots also show increased variability in AP firing in isolated SAN myocytes from AngII-infused mice (Figure 6F), which was reduced in the presence of ISO (Figure 6G). ISO reduced SD1 and SD2 in both groups, but variability was still larger in AngII-infused mice (Figures 6H and 6I).

CCh increased IBI in isolated SAN myocytes from both saline- and AngII-infused mice (Figures 7A and 7B); however, the change in IBI was smaller in AngII-infused mice (Figure 7C). CCh increased SDNN and COV in isolated SAN myocytes from saline- and AngII-infused mice; however, these effects were smaller in AngII-infused mice and there were no differences in SDNN or COV between saline- and AngII-infused mice in the presence of CCh (Figures 7D and 7E). Poincaré plots further confirm the blunted effects of CCh on AP firing variability in AngII-infused mice (Figures 7F and 7G). SD1 and SD2 were increased with the application of CCh in both groups, but the increase in variability was less in AngII-infused mice (Figures 7H and 7I). Thus, the effects of ANS agonists (ISO and CCh) on spontaneous AP firing in SAN myocytes are impaired after AngII infusion.

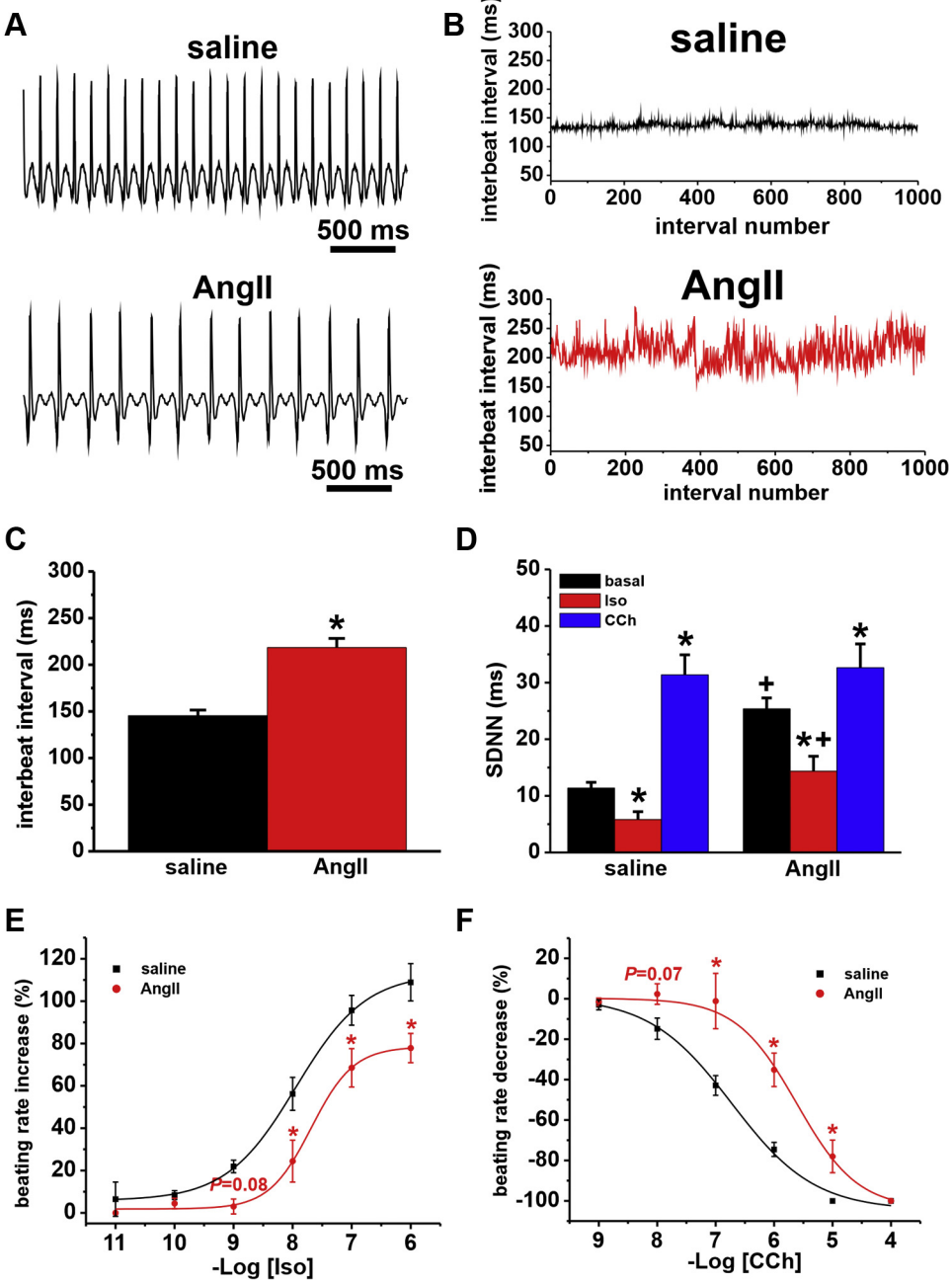

Figure 5 Beating rate variability and effects of autonomic nervous system (ANS) agonists in isolated atrial preparations from Angiotensin II (AngII)-infused mice. **A:** Representative electrograms in isolated atrial preparations from saline- and AngII-infused mice. **B:** Representative tachograms from isolated atrial preparations from saline- and AngII-infused mice. **C:** Effects of AngII on interbeat interval in isolated atrial preparations. *$P<.05$ vs saline by Student *t* test. **D:** Summary of the effects of isoproterenol (ISO, 10 nM) and carbachol (CCh, 10 nM) on standard deviation of N-N interval (SDNN) in isolated atrial preparations from saline- and AngII-infused mice. *$P<.05$ vs basal condition within treatment group; $^{+}P<.05$ vs saline within drug condition by 2-way analysis of variance (ANOVA) with a Holm-Sidak post hoc test. **E and F:** Dose-response curves demonstrating the effects of ISO (panel E) and CCh (panel F) on beating rate in atrial preparations isolated from saline- and AngII-infused mice. *$P<.05$ vs saline by 2-way repeated measures ANOVA with a Hold-Sidak post hoc test. n=12 saline-infused mice and n=12 AngII-infused mice for basal conditions; n=6 saline-infused mice and n=6 AngII-infused mice for ISO injection studies; and n=5 saline-infused mice and n=5 AngII-infused mice for CCh injection studies.

Discussion

HRV has been used to assess changes in ANS activity in hypertensive patients; however, prior studies have not adequately considered the possibility that changes in intrinsic SAN function may also affect HRV in hypertension. Accordingly, the goal of the present study was to assess the contributions of changes in ANS activity, responsiveness of the SAN to ANS agonists, and changes in intrinsic SAN function to altered HRV in hypertension. We found that HRV is reduced in AngII-infused mice, which is highly consistent with reductions in HRV seen in human patients with hypertension.[8,9] Our study demonstrates that hypertension due to AngII

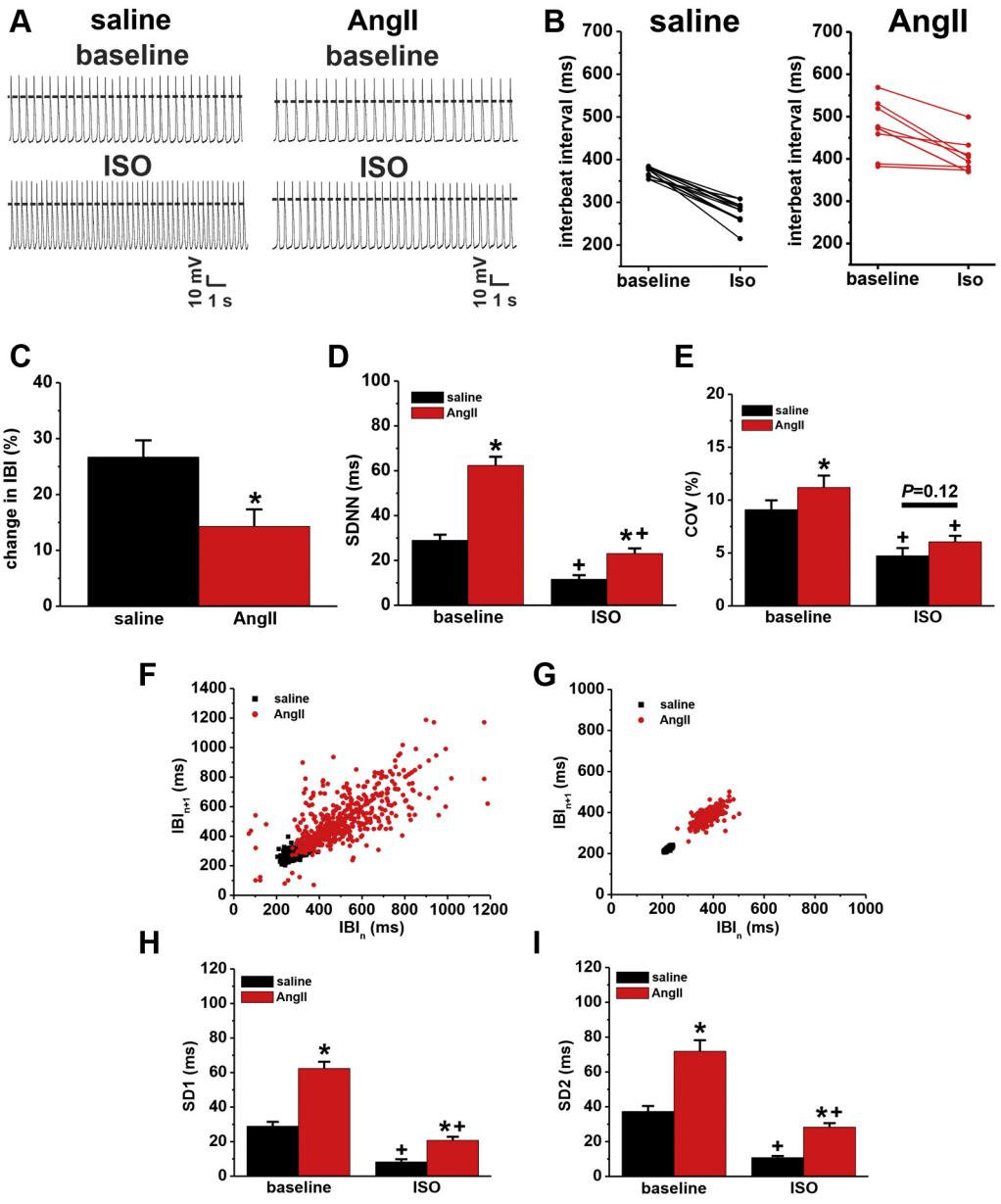

Figure 6 Effect of isoproterenol (ISO) on interbeat interval (IBI) and beating rate variability in isolated sinoatrial node (SAN) myocytes from saline- and Angiotensin II (AngII)-infused mice. **A:** Representative spontaneous action potential (AP) recordings in isolated SAN myocytes from saline- and AngII-infused mice at baseline and after the application of ISO (1 μM). **B:** IBI in isolated SAN myocytes from saline- and AngII-infused mice at baseline and ISO (1 μM). **C–E:** Summary of the change in beating interval (panel C), standard deviation of N-N intervals (SDNN) (panel D), and the coefficient of variation (COV) (panel E) in isolated SAN myocytes from saline- and AngII-infused mice at baseline and in the presence of ISO (1 μM). For panel C *$P<.05$ vs saline by Student *t* test; for panels D and E *$P<.05$ vs saline; +$P<.05$ vs baseline by 2-way analysis of variance (ANOVA) with Holm-Sidak posthoc test. n=7 SAN myocytes from saline-infused mice and n=9 SAN myocytes from AngII-infused mice. **F and G:** Representative Poincaré plots from spontaneous AP recordings in isolated SAN myocytes from saline- and AngII-infused mice at baseline (panel F) and in ISO (panel G). **H and I:** Summary of the effects of ISO on SD1 (panel H) and SD2 (panel I) in isolated SAN myocytes from saline- and AngII-infused mice. *$P<.05$ vs saline; $^{+}P<.05$ vs baseline by 2-way ANOVA with Holm-Sidak post hoc test. n=7 SAN myocytes from saline-infused mice and n=9 SAN myocytes from AngII-infused mice.

infusion leads to reduced HRV in association with changes in ANS activity (ie, altered sympathovagal balance), impaired responsiveness of the SAN to β-AR and M_2 receptor stimulation, and alterations in intrinsic SAN beating interval variability. Our findings strongly support the concept that HRV should not be interpreted only in relation to changes in ANS activity.[3] Rather, our study shows that HRV arises from complex interactions between the ANS and the SAN, depending on intrinsic properties of both regions, as well as the interactions between the 2 via autonomic neurotransmitters. Our approach of analyzing HRV at multiple levels (in vivo to isolated SAN myocytes) provides new insight into the specific contributions of the ANS and the SAN to changes in HRV in hypertension.

SNS dysfunction has been well described in hypertension.[13–16] Consistent with this, our assessment of HRV

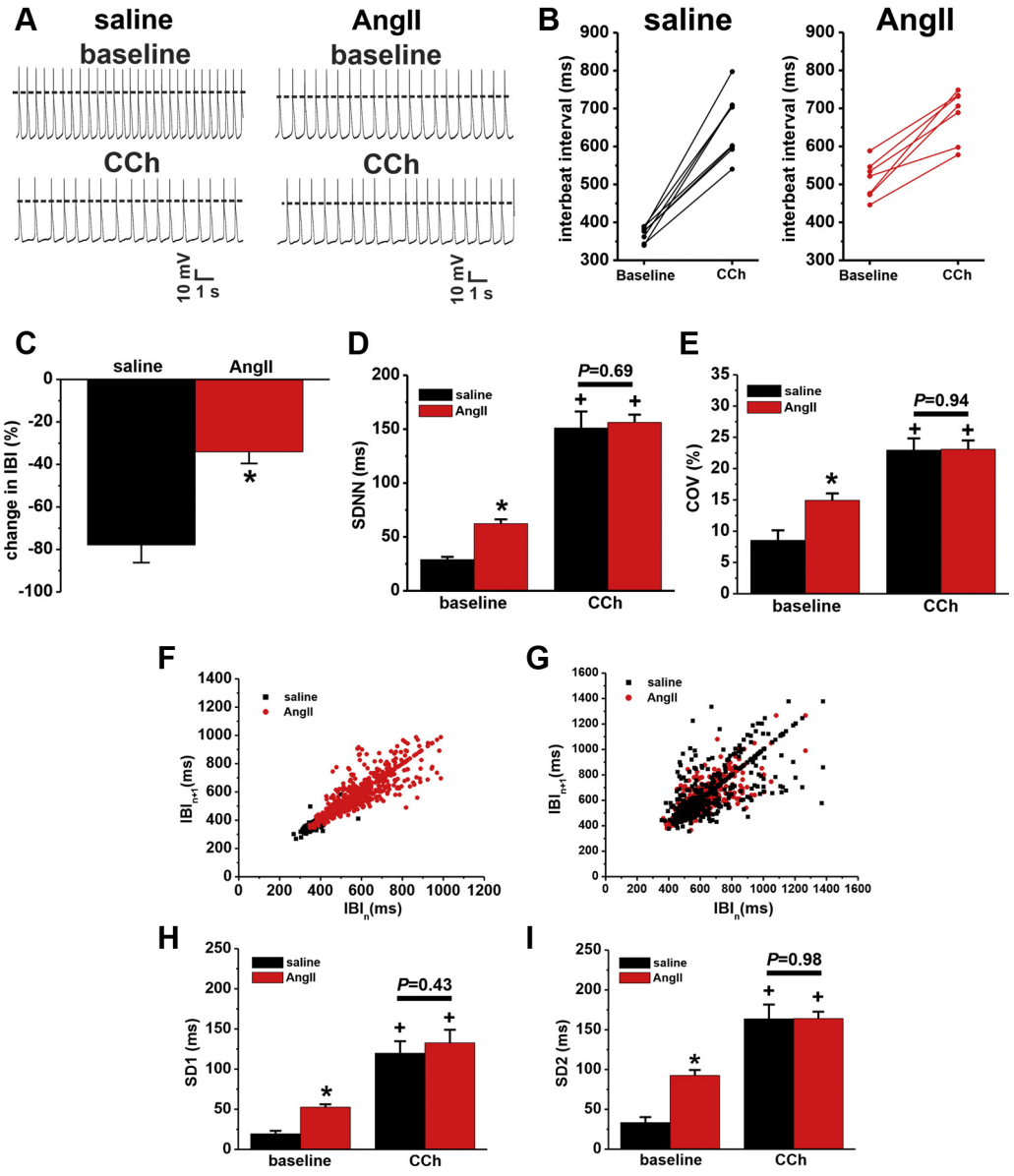

Figure 7 Effect of carbachol (CCh) on interbeat interval (IBI) and beating rate variability in isolated sinoatrial node myocytes from saline- and Angiotensin II (AngII)-infused mice. **A:** Representative spontaneous action potential (AP) recordings in isolated SAN myocytes from saline- and AngII-infused mice at baseline and after the application of CCh (50 nM). **B:** IBI in isolated SAN myocytes from saline- and AngII-infused mice at baseline and CCh (50 nM). **C–E:** Change in beating interval (panel C), standard deviation of N-N intervals (SDNN) (panel D), and the coefficient of variation (COV) (panel E) in isolated SAN myocytes from saline- and AngII-infused mice at baseline and in the presence of CCh (50 nM). For panel C *P<.05 vs saline by Student t test; for panels D and E *P<.05 vs saline; +P<.05 vs baseline by 2-way analysis of variance (ANOVA) with Holm-Sidak posthoc test. n=8 SAN myocytes from saline-infused mice and n=7 SAN myocytes from AngII-infused mice. **F and G:** Representative Poincaré plots from spontaneous AP recordings in isolated SAN myocytes from saline- and AngII-infused mice at baseline (panel F) and in CCh (panel G). **H and I:** Summary of the effects of CCh on SD1 (panel H) and SD2 (panel I) in isolated SAN myocytes from saline- and AngII-infused mice. *P<.05 saline; ^{+}P<.05 vs baseline by 2-way ANOVA with Holm-Sidak post hoc test. n=8 SAN myocytes from saline-infused mice and n=7 SAN myocytes from AngII-infused mice.

from time and frequency domain analysis in vivo indicates a shift toward enhanced SNS activity in AngII-infused mice. Furthermore, we found that SNS activity was enhanced in AngII-infused mice while responsiveness of the SAN, including at the level of the SAN myocyte, to β-AR agonists was reduced. Consistent with these observations, AngII-infused mice showed greater HR increases after β-AR blockade with propranolol and elevated plasma norepinephrine levels, which is similar to the findings reported in human patients with hypertension.[14,16] Thus, it is a combination of the change in sympathovagal balance and sensitivity of the SAN myocytes to ANS transmitters that collectively determines how the ANS affects HR and HRV in AngII-mediated hypertension. Chronically elevated SNS activity is thought to lead to β-AR desensitization, which can lead to a loss of chronotropic and inotropic reserve.[14,17]

PNS dysfunction has also been described in hypertensive patients[14]; however, the basis for this is less well understood. Evidence for PNS dysfunction is often derived from in vivo HRV assessment (RMSSD and HF power are both thought to be indicators of PNS function[10,18]) or measurements of HR after the administration of the M_2 receptor blocker atropine.[19,20] Using these approaches, we found that RMSSD, HF power, and the magnitude of the effect of atropine on HR were each reduced in AngII-infused mice. While some studies in canine models have reported increases in vagal nerve activity in overt HF,[21,22] we observed no alterations in vagal nerve activity in AngII-mediated hypertension. Prior studies have also attributed a reduction in the HF component of HRV to parasympathetic withdrawal.[20,23] We found that a critical determinant of parasympathetic dysfunction in AngII-mediated hypertension is the impaired effects of CCh on HR and SAN myocyte beating rate at the level of the SAN myocyte. Our findings in AngII-infused mice demonstrate that impaired responsiveness of the SAN to M_2 receptor stimulation can underlie PNS dysfunction in hypertension.

Several recent studies demonstrate that alterations in the intrinsic properties of the SAN during aging[24] or in disease states[3,5] can alter HRV in vivo in conjunction with changes in ANS activity. Our present investigations in hypertension are highly consistent with these other studies in demonstrating that intrinsic changes in beating interval variability in the isolated SAN and in isolated SAN myocytes contribute importantly to overall HRV in vivo. Specifically, AngII infusion results in increased IBI (ie, reduced beating rate) and enhanced beating interval variability in intact, denervated atrial preparations and in isolated SAN myocytes, which are evidence for intrinsic SAN dysfunction. This is consistent with the increased occurrence of sinus pauses observed in vivo in AngII-infused mice. Interestingly, despite the presence of overt SAN dysfunction, AngII-infused mice were found to exhibit elevated HR when assessed in the conscious, freely moving state by telemetry. This is likely due to the increased SNS activity in AngII-induced hypertension. Thus, the change in sympathovagal balance observed in vivo in AngII-infused mice may be compensating for the reduced intrinsic HR; however, this increase in SNS activity, along with the changes in sensitivity of SAN myocytes to ANS agonists, also leads to an overall reduction in HRV. Prior studies have shown that elevated AngII leads to SNS activation in hypertension.[15] Furthermore, elevated HR and tachycardia are frequently associated with hypertension.[14,25] These elevations in HR are associated with worse long-term survival,[23] which may be related to issues with enhanced SNS activity attempting to compensate for intrinsic SAN dysfunction leading to reduced HRV.

We have previously shown that SAN dysfunction in AngII-mediated hypertension occurs in association with impaired spontaneous AP generation in SAN myocytes due to the reduction in the hyperpolarization-activated current (I_f) and reduced expression of the *HCN4* gene.[7] We also found that AngII infusion leads to elevated SAN fibrosis, which can further impair conduction in the SAN.[26] These alterations may be important contributors to the increased variability in SAN spontaneous AP firing in AngII-mediated hypertension. Additional studies will be required to further determine these relationships.

While our studies clearly demonstrate that the responsiveness of the SAN to SNS and PNS agonists is impaired, the basis for this is not well understood. There are a number of possible mechanisms that could explain these observations, including desensitization of β-AR and M_2 receptors, changes in receptor expression, and/or changes in the expression or regulation of important downstream signaling molecules in these pathways (ie, G proteins, adenylyl cyclases, kinases, phosphodiesterases, and others). This will be an important avenue for ongoing investigation.

Some additional limitations of our study should be noted. Our studies were performed in mice, which have differences in HR, ANS activity, and HRV compared to humans. Similarly, there may be differences in these parameters in different strains of mice.[27,28] Thus, it will be important to conduct additional studies in other animal models and in human patients.

Conclusion

This study provides a comprehensive multilevel assessment of ANS and SAN function in mice with AngII-induced hypertensive heart disease. Our data demonstrate that the origins of reduced HRV in the setting of hypertension arise from both neural factors and intrinsic SAN dysfunction. Reduced responses to M_2 receptor stimulation in conjunction with enhanced SNS activation and commensurate β-AR desensitization collectively result in higher resting HRs and reduced HRV, a combination that likely contributes to the progression of cardiac dysfunction in hypertension. This work highlights the importance of considering the activity of the ANS, the signaling between the ANS and the SAN, as well as intrinsic SAN function when interpreting HRV.

Acknowledgments

We acknowledge Adam Kirkby, MSc for assistance with mouse surgeries.

Appendix

Supplementary data

Supplementary data associated with this article can be found in the online version at https://doi.org/10.1016/j.hrthm.2020.03.014.

References

1. Mangoni ME, Nargeot J. Genesis and regulation of the heart automaticity. Physiol Rev 2008;88:919–982.
2. Billman GE. Heart rate variability—a historical perspective. Front Physiol 2011;2:86.
3. Yaniv Y, Lyashkov AE, Lakatta EG. Impaired signaling intrinsic to sinoatrial node pacemaker cells affects heart rate variability during cardiac disease. J Clin Trials 2014;4.

4. Hillebrand S, Gast KB, de Mutsert R, et al. Heart rate variability and first cardiovascular event in populations without known cardiovascular disease: meta-analysis and dose-response meta-regression. Europace 2013;15:742–749.
5. Papaioannou VE, Verkerk AO, Amin AS, et al. Intracardiac origin of heart rate variability, pacemaker funny current and their possible association with critical illness. Curr Cardiol Rev 2013;9:82–96.
6. Jensen PN, Gronroos NN, Chen LY, et al. Incidence of and risk factors for sick sinus syndrome in the general population. J Am Coll Cardiol 2014;64:531–538.
7. Mackasey M, Egom EE, Jansen HJ, et al. Natriuretic peptide receptor-C protects against angiotensin II-mediated sinoatrial node disease in mice. JACC Basic Transl Sci 2018;3:824–843.
8. Schroeder EB, Liao D, Chambless LE, et al. Hypertension, blood pressure, and heart rate variability: the Atherosclerosis Risk in Communities (ARIC) study. Hypertension 2003;42:1106–1111.
9. Virtanen R, Jula A, Kuusela T, et al. Reduced heart rate variability in hypertension: associations with lifestyle factors and plasma renin activity. J Hum Hypertens 2003;17:171–179.
10. Moghtadaei M, Langille E, Rafferty SA, et al. Altered heart rate regulation by the autonomic nervous system in mice lacking natriuretic peptide receptor C (NPR-C). Sci Rep 2017;7:17564.
11. Azer J, Hua R, Krishnaswamy PS, et al. Effects of natriuretic peptides on electrical conduction in the sinoatrial node and atrial myocardium of the heart. J Physiol 2014;592:1025–1045.
12. Rose RA, Lomax AE, Kondo CS, et al. Effects of C-type natriuretic peptide on ionic currents in mouse sinoatrial node: a role for the NPR-C receptor. Am J Physiol Heart Circ Physiol 2004;286:H1970–H1977.
13. Thayer JF, Yamamoto SS, Brosschot JF. The relationship of autonomic imbalance, heart rate variability and cardiovascular disease risk factors. Int J Cardiol 2010;141:122–131.
14. Mancia G, Grassi G. The autonomic nervous system and hypertension. Circ Res 2014;114:1804–1814.
15. Grassi G, Seravalle G, Mancia G. Sympathetic activation in cardiovascular disease: evidence, clinical impact and therapeutic implications. Eur J Clin Invest 2015;45:1367–1375.
16. Castellano M, Bohm M. The cardiac beta-adrenoceptor-mediated signaling pathway and its alterations in hypertensive heart disease. Hypertension 1997; 29:715–722.
17. Izzo R, Cipolletta E, Ciccarelli M, et al. Enhanced GRK2 expression and desensitization of betaAR vasodilatation in hypertensive patients. Clin Transl Sci 2008;1:215–220.
18. Fenske S, Probstle R, Auer F, et al. Comprehensive multilevel in vivo and in vitro analysis of heart rate fluctuations in mice by ECG telemetry and electrophysiology. Nat Protoc 2016;11:61–86.
19. Dunlap ME, Bibevski S, Rosenberry TL, et al. Mechanisms of altered vagal control in heart failure: influence of muscarinic receptors and acetylcholinesterase activity. Am J Physiol Heart Circ Physiol 2003;285:H1632–H1640.
20. Olshansky B, Sabbah HN, Hauptman PJ, et al. Parasympathetic nervous system and heart failure: pathophysiology and potential implications for therapy. Circulation 2008;118:863–871.
21. Chan YH, Tsai WC, Shen C, et al. Subcutaneous nerve activity is more accurate than heart rate variability in estimating cardiac sympathetic tone in ambulatory dogs with myocardial infarction. Heart Rhythm 2015;12:1619–1627.
22. Piccirillo G, Ogawa M, Song J, et al. Power spectral analysis of heart rate variability and autonomic nervous system activity measured directly in healthy dogs and dogs with tachycardia-induced heart failure. Heart Rhythm 2009; 6:546–552.
23. van Bilsen M, Patel HC, Bauersachs J, et al. The autonomic nervous system as a therapeutic target in heart failure: a scientific position statement from the Translational Research Committee of the Heart Failure Association of the European Society of Cardiology. Eur J Heart Fail 2017;19:1361–1378.
24. Yaniv Y, Ahmet I, Tsutsui K, et al. Deterioration of autonomic neuronal receptor signaling and mechanisms intrinsic to heart pacemaker cells contribute to age-associated alterations in heart rate variability in vivo. Aging Cell 2016; 15:716–724.
25. Palatini P. Role of elevated heart rate in the development of cardiovascular disease in hypertension. Hypertension 2011;58:745–750.
26. Csepe TA, Kalyanasundaram A, Hansen BJ, et al. Fibrosis: a structural modulator of sinoatrial node physiology and dysfunction. Front Physiol 2015;6:37.
27. Shusterman V, Usiene I, Harrigal C, et al. Strain-specific patterns of autonomic nervous system activity and heart failure susceptibility in mice. Am J Physiol Heart Circ Physiol 2002;282:H2076–H2083.
28. Shah AP, Siedlecka U, Gandhi A, et al. Genetic background affects function and intracellular calcium regulation of mouse hearts. Cardiovasc Res 2010; 87:683–693.

Altered heart rate variability in Angiotensin II mediated hypertension is associated with impaired autonomic nervous system signaling and intrinsic sinoatrial node dysfunction

Supplemental Material

Supplemental Methods

Mice

This study used male wildtype C57Bl/6 mice between the ages of 10–15 weeks. Mice were treated with saline or AngII (2.5 mg/kg/day) for 3 weeks using osmotic minipumps (Alzet). To implant osmotic pumps mice were anesthetized by isoflurane inhalation (2%). Osmotic pumps were then inserted subcutaneously via a mid-scapular incision, as we have described previously.[1,2] Blood pressure was measured at baseline (i.e. before pump insertion) and at the end of the 3 week treatment period by tail-cuff plethysmography, as we have done previously.[1,2]

Telemetry studies

Telemetric recordings (HD-X11 telemeters, Data Sciences International) were used to measure ECGs and activity levels in conscious freely moving mice. ECG leads were positioned subcutaneously in a lead II position to continuously measure HR as we have previously described.[3] Telemeters were inserted at the same time as osmotic pumps. At the end the 3 week saline or AngII infusion period, 48 hrs of baseline ECG recording was obtained. Following this 48 hr recording period, the effects of ANS blockade were investigated by intraperitoneal injection of the β-adrenergic receptor (β-AR) antagonist propranolol hydrochloride (10 mg/kg) and the muscarinic receptor antagonist atropine sulfate (10 mg/kg) alone or in combination with a minimum of 24 hrs between injections. ECGs were recorded continuously for 1 hr following drug injection. All studies were performed in an electrically shielded telemetry room ensuring a quiet and undisturbed environment for the mice used in these experiments. ECG data

acquisition, ECG filtering and R-wave detection was done using Ponemah software (Data Sciences International).

Vagal parasympathetic and renal sympathetic nerve recordings

After 3 weeks of saline or AngII infusion, mice were anesthetized using isoflurane (5% induction, 1.5-2% maintenance) in 100% oxygen. Core body temperature was measured using a rectal probe and maintained at 37°C using a heated surgical pad. Renal sympathetic nerve activity (RSNA) recordings were measured by multifiber recording directly from the renal nerve. The renal neurovascular bundle was visualized with a high-power dissecting microscope and the renal nerve was dissected free from connective tissue using fine tipped forceps. The nerve was then placed on a custom-made bipolar silver wire electrode to record activity. Vagal nerve activity (VNA) recordings from the right cervical vagus were obtained in the same fashion. Mice were then euthanized by isoflurane overdose and nerve activity was recorded to estimate background noise. Nerve bursts were classified as any signal above the background noise threshold. Nerve signals were sampled at 4 kHz with a digital amplifier (Dual Bio Amp; AD Instruments) and displayed in real time during the procedure. The raw signal was then high-pass filtered at 300 Hz and analyzed offline using Lab Chart 8 (Spike Analysis Module). Firing frequency was calculated as the total number of spikes over the 10 min recording.

Atrial preparation

Mice were administered a 0.2 ml intraperitoneal injection of heparin (1000 IU/ml) to prevent blood clotting and were then anesthetized by isoflurane inhalation and cervically dislocated. Hearts were rapidly excised into Krebs solution (37°C) containing (in mM): 118 NaCl, 4.7 KCl, 1.2 KH_2PO_4, 12.2 $MgSO_4$, 1 $CaCl_2$, 25 $NaHCO_3$, 11 glucose. This Krebs solution was bubbled with 95% O_2/5% CO_2 in order to maintain a pH of 7.4. The atria were dissected away from the ventricles and pinned in a dish with the endocardial surface facing upwards. The

superior and inferior vena cavae were cut open so that the crista terminalis and the right atrial posterior wall, which contains the SAN, could be visualized. These atrial preparations were given a minimum of 15 min to equilibrate before data were collected.

Patch-clamping of isolated SAN myocytes

The procedures for isolating single pacemaker myocytes from the sinoatrial node (SAN), of the mouse have been described previously[4,5] and were as follows. Mice were administered a 0.2 ml intraperitoneal injection of heparin (1000 IU/ml) to prevent blood clotting. Following this, mice were anesthetized by isoflurane inhalation and then euthanized by cervical dislocation. The heart was excised into Tyrode's solution (35ºC) consisting of (in mmol/L) 140 NaCl, 5.4 KCl, 1.2 KH_2PO_4, 1.0 $MgCl_2$, 1.8 $CaCl_2$, 5.55 glucose, and 5 HEPES, with pH adjusted to 7.4 with NaOH. The sinoatrial node (SAN) region of the heart was isolated by separating the atria from the ventricles, cutting open the superior and inferior venae cavae, and pinning the tissue so that the crista terminalis could be identified. The SAN area is located in the intercaval region adjacent to the crista terminalis. This SAN region was cut into strips, which were transferred and rinsed in a 'low Ca^{2+}, Mg^{2+} free' solution containing (in mmol/L) 140 NaCl, 5.4 KCl, 1.2 KH_2PO_4, 0.2 $CaCl_2$, 50 taurine, 18.5 glucose, 5 HEPES and 1 mg/ml bovine serum albumin (BSA), with pH adjusted to 6.9 with NaOH. SAN tissue strips were digested in 5 ml of 'low Ca^{2+}, Mg^{2+} free' solution containing collagenase (type II, Worthington Biochemical Corporation), elastase (Worthington Biochemical Corporation) and protease (type XIV, Sigma Chemical Company) for 30 min. Then the tissue was transferred to 5 ml of modified KB solution containing (in mmol/L) 100 potassium glutamate, 10 potassium aspartate, 25 KCl, 10 KH_2PO_4, 2 $MgSO_4$, 20 taurine, 5 creatine, 0.5 EGTA, 20 glucose, 5 HEPES, and 0.1% BSA, with pH adjusted to 7.2 with KOH. The tissue was mechanically agitated using a wide-bore pipette. This procedure yielded individual SAN myocytes with cellular automaticity that was recovered after readapting the cells to a physiological concentration of Ca^{2+}. SAN myocytes were identified by their small spindle

shape and ability to beat spontaneously in the recording chamber when superfused with normal Tyrode's solution. When patch-clamped, SAN myocytes displayed spontaneous action potentials. The capacitance of single SAN myocytes was 20 – 35 pF.

Spontaneous action potentials (APs) were recorded using the perforated patch-clamp technique on single SAN myocytes. For recording APs the recording chamber was superfused with a normal Tyrode's solution (22 – 23ºC) containing (in mmol/L) 140 NaCl, 5 KCl, 1 $MgCl_2$, 1 $CaCl_2$, 10 HEPES, and 5 glucose, with pH adjusted to 7.4 with NaOH. The pipette filling solution for I_f contained (in mmol/L) 135 KCl, 0.1 $CaCl_2$, 1 $MgCl_2$, 5 NaCl, 10 EGTA, 4 Mg-ATP, 6.6 Na-phosphocreatine, 0.3 Na-GTP and 10 HEPES, with pH adjusted to 7.2 with KOH. Amphotericin B (200 µg/ml) was added to this pipette solution to record APs with the perforated patch clamp technique. APs and membrane currents were recorded at room temperature (22-23℃), which must be noted when comparing AP frequency in isolated cells to beating rates *in vivo* or in isolated hearts at body temperature.

Micropipettes were pulled from borosilicate glass (with filament, 1.5 mm OD, 0.75 mm ID, Sutter Instrument Company) using a Flaming/Brown pipette puller (model p-87, Sutter Instrument Company). The resistance of these pipettes was 4 – 8 MΩ when filled with recording solution. Micropipettes were positioned with a micromanipulator (Burleigh PCS-5000 system) mounted on the stage of an inverted microscope (Olympus IX71). Seal resistance was 2 – 15 GΩ. For perforated patch clamp experiments access resistance was monitored for the development of capacitative transients upon sealing to the cell membrane with Amphotericin B in the pipette. Typically, access resistance became less than 30 MΩ within 5 min of sealing onto the cell, which was sufficient for recording spontaneous APs in current clamp mode. Data were digitized using a Digidata 1440 and pCLAMP 10 software (Molecular Devices) and stored on computer for *post hoc* analysis.

HRV analysis

HRV was assessed using time and frequency domain analysis from telemetric ECG recordings *in vivo* and were analyzed as we have described previously.[3] Briefly, 12 hr segments of light and dark (day/night) phases were selected from the complete recording period and were analyzed separately. For R-wave detection, each 12 hr segment was divided into six 2 hr segments. Low and high-activity phases were separated within the light and dark segments based on activity measured from telemeters. Each episode was examined to ensure a stationary and stable sinus rhythm. R-wave detection was then performed, and the RR-interval time series was obtained.

In isolated atrial preparations and isolated SAN myocytes, N-N intervals were defined as the interval between peaks on the electrogram recordings in atrial preparations or spontaneous APs in SAN myocytes, respectively. Stationary N-N interval time series of at least 5 min in duration were used for time domain analysis.

For time domain analysis, each of the day/night, low/high-activity phases were divided into 10 min episodes. Each episode was examined to ensure a stationary and stable sinus rhythm with no trend or periodic fluctuations. Next, R-wave detection was performed and R-R interval time series were obtained. The time domain parameters we are reporting include the standard deviation of all normal R–R intervals (SDNN, in ms) and the root mean square differences between successive R-R intervals (RMSSD, in ms).

For frequency domain analysis, each of the day/night, low/high-activity phases were divided into 2 min episodes. These time frames were chosen in order to ensure that each episode contained at least 1024 data points (R waves). Similar to the time domain analysis, each episode was manually examined to ensure a stationary and stable sinus rhythm, which is required for performing fast Fourier transforms (see below). Next, R-wave detection was performed and the R-R interval time series were generated. Linear trends and drift were removed from the signal to reveal the HRV in the data. In the present study, we have used Welch's method to characterize the frequency content of the signal, i.e. to estimate the power of

the signal at different frequencies[6]. In Welch's method, the signal is broken into overlapping segments to reduce noise in the frequency spectrum. Then, the segments are windowed to reduce spectral leakage. The periodogram of each windowed segment is calculated using the Fourier transform. Finally, the periodograms are averaged to make a single frequency spectrum. In the present study, we have used 50% overlapping and the Hamming window for the spectral density estimation.[7] All data were analyzed using customized software written in Matlab version 9.1 software (Mathworks) as we have described previously.[3]

The total power of each periodogram was measured as a total index of HRV, which determines the integral of total variability over the entire frequency range. Then, the high frequency (HF) and low frequency (LF) components were extracted. The HF component of HRV (1.5–5 Hz) is predominantly mediated by the phasic activity of the parasympathetic nervous system.[8] The LF oscillations of HR (0.1–1.5 Hz) are regulated by both the sympathetic and parasympathetic nervous systems; however, the tonic sympathetic component is dominant.[8]

Beating interval variability was also assessed using non-linear metrics from Poincaré plot analysis. From these the standard deviations (SD1 and SD2) were calculated using the following equations: $SD1^2=1/2[SD(RR_n-RR_{n+1})]^2$ and $SD2^2=2[SD(RR)]^2-1/2[SD(RR_n-RR_{n+1})]^2$.

Supplemental Results

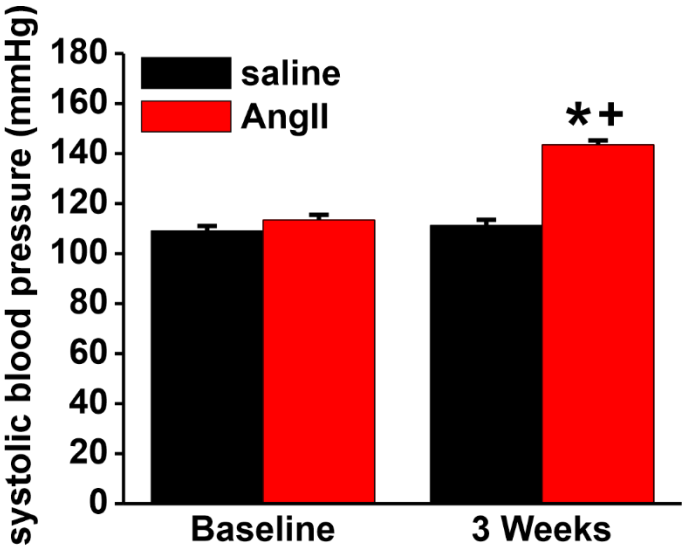

Figure S1: Systolic blood pressure in AngII infused mice. Blood pressure was measured at baseline and after 3 weeks of infusion with saline or AngII. *P<0.001 vs. baseline within treatment group, ^{+}P<0.001 vs. saline at 3 week time point. Data analyzed by two-way ANOVA with Tukey's posthoc test; n=8 mice per group.

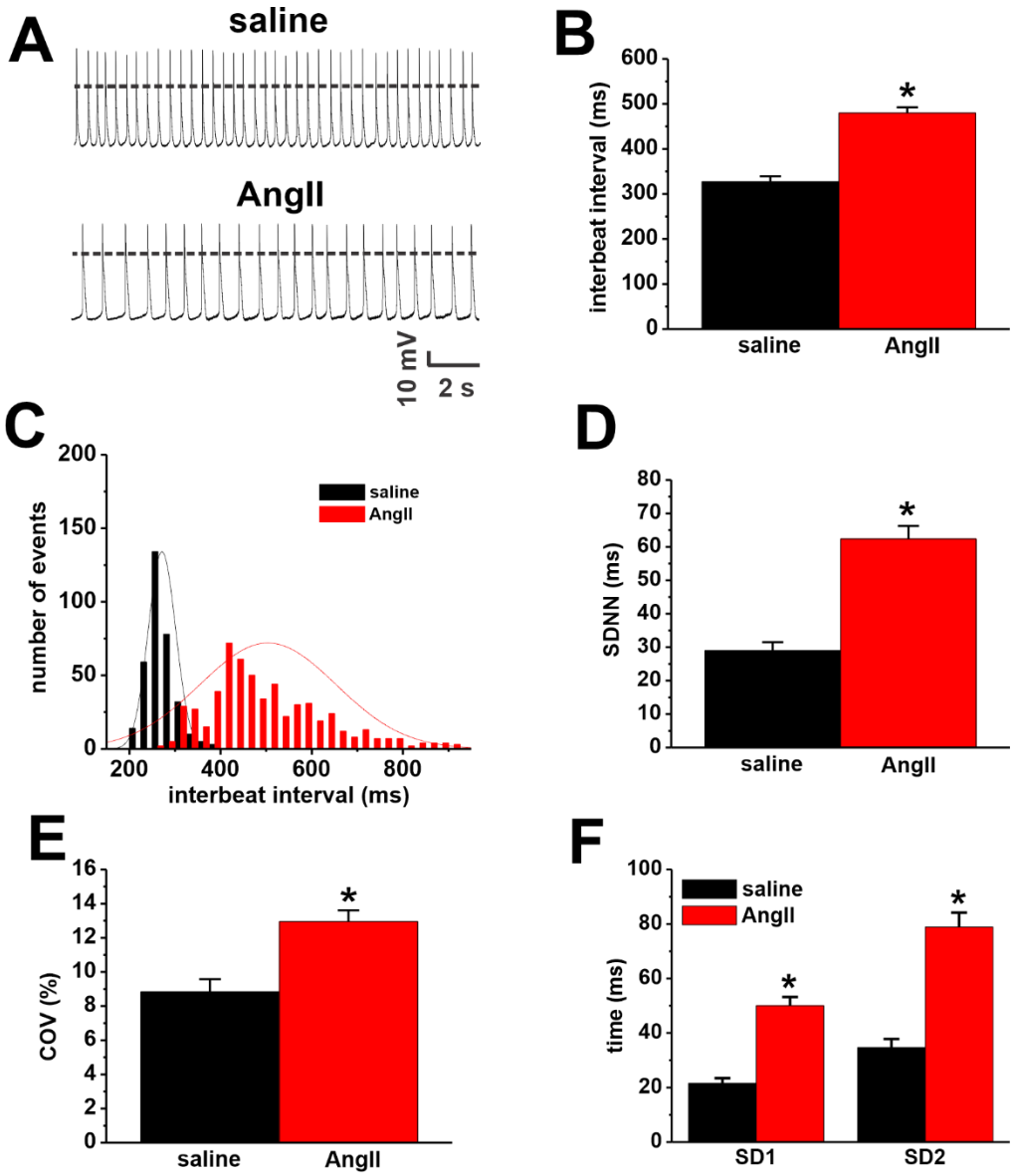

Supplemental Figure S2: Assessment of beating rate variability in isolated SAN myocytes from saline and AngII infused mice. (**A**) Representative spontaneous action potential recordings in isolated SAN myocytes from saline and AngII infused mice. (**B**) Interbeat interval (IBI) in isolated SAN myocytes from saline and AngII infused mice. (**C**) Summary histograms for interbeat interval intervals from spontaneous AP recordings in isolated SAN myocytes from saline and AngII infused mice. (**D**) SDNN for spontaneous AP firing in isolated SAN myocytes from saline and AngII infused mice. (**E**) Coefficient of variation for spontaneous AP firing in isolated SAN myocytes from saline and AngII infused mice. (**F**) SD1 and SD2 for spontaneous AP firing in isolated SAN myocytes from saline and AngII infused mice. *P<0.05 vs. saline by Student's t-test; n=19 SAN myocytes from saline infused mice and 20 SAN myocytes from AngII infused mice. Data compiled from recordings presented in Figures 6 and 7 in main manuscript.

References

1. Mackasey M, Egom EE, Jansen HJ, et al. Natriuretic Peptide Receptor-C Protects Against Angiotensin II-Mediated Sinoatrial Node Disease in Mice. JACC Basic Transl Sci 2018;3:824-843.
2. Jansen HJ, Mackasey M, Moghtadaei M, et al. NPR-C (Natriuretic Peptide Receptor-C) Modulates the Progression of Angiotensin II-Mediated Atrial Fibrillation and Atrial Remodeling in Mice. Circ Arrhythm Electrophysiol 2019;12:e006863.
3. Moghtadaei M, Langille E, Rafferty SA, et al. Altered heart rate regulation by the autonomic nervous system in mice lacking natriuretic peptide receptor C (NPR-C). Sci Rep 2017;7:17564.
4. Springer J, Azer J, Hua R, et al. The natriuretic peptides BNP and CNP increase heart rate and electrical conduction by stimulating ionic currents in the sinoatrial node and atrial myocardium following activation of guanylyl cyclase-linked natriuretic peptide receptors. J Mol Cell Cardiol 2012;52:1122-1134.
5. Egom EE, Vella K, Hua R, et al. Impaired sinoatrial node function and increased susceptibility to atrial fibrillation in mice lacking natriuretic peptide receptor C. J Physiol 2015;593:1127-1146.
6. Welch P. The use of fast Fourier transform for the estimation of power spectra: A method based on time averaging over short, modified periodograms. IEEE Transactions on Audio and Electroacoustics 1967;15:70-73.
7. Alessio SM. Digital Signal Processing and Spectral Analysis for Scientists: Concepts and Applications: Springer International Publishing; 2015.
8. Fenske S, Probstle R, Auer F, et al. Comprehensive multilevel in vivo and in vitro analysis of heart rate fluctuations in mice by ECG telemetry and electrophysiology. Nat Protoc 2016;11:61-86.